Supplement of Clim. Past, 19, 61–85, 2023
https://doi.org/10.5194/cp-19-61-2023-supplement

Climate of the Past
Open Access
EGU

Supplement of

Unraveling the mechanisms and implications of a stronger mid-Pliocene Atlantic Meridional Overturning Circulation (AMOC) in PlioMIP2

Julia E. Weiffenbach et al.

Correspondence to: Julia E. Weiffenbach (j.e.weiffenbach@uu.nl)

Supplementary Tables and Figures

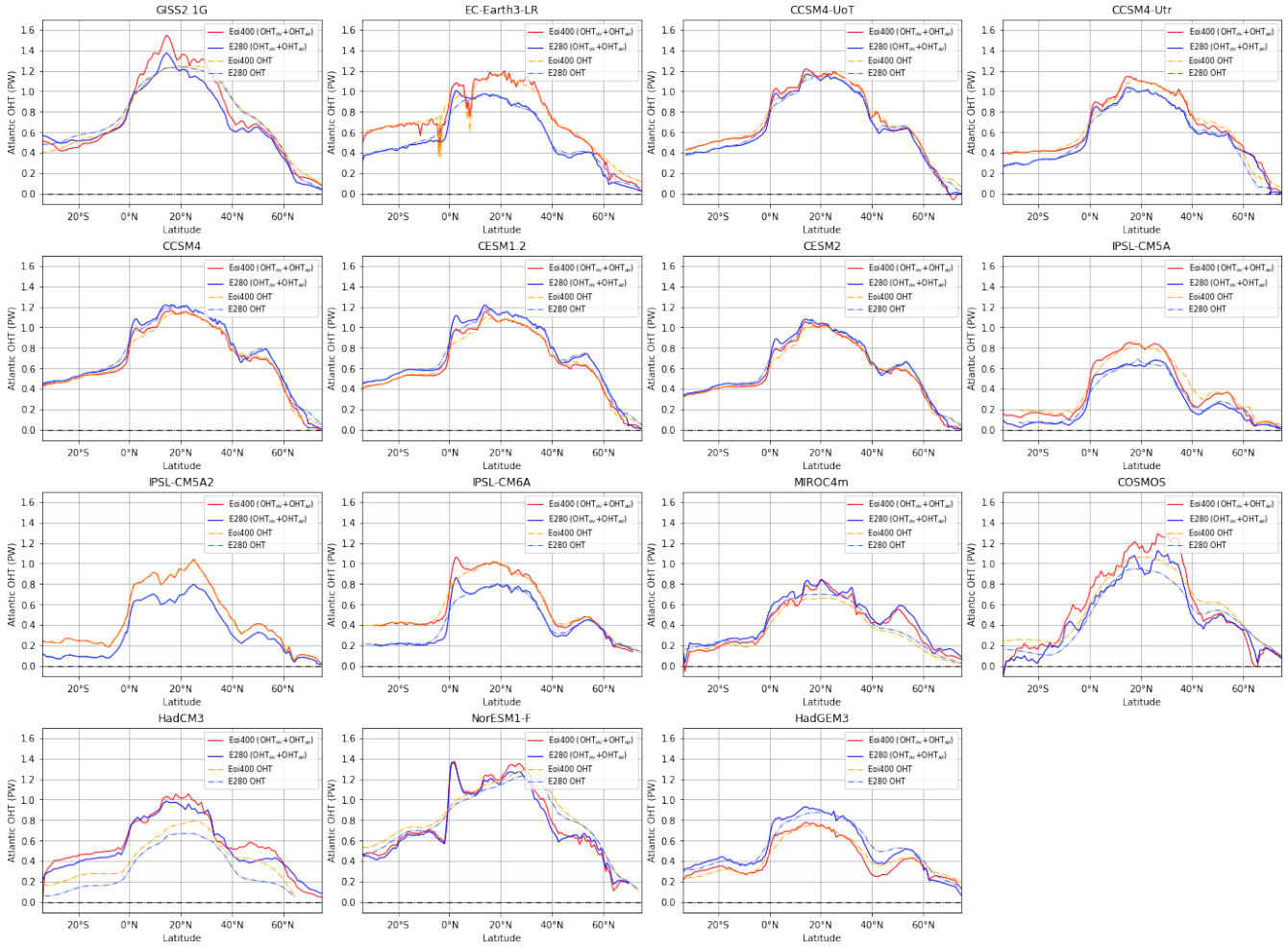

Figure S1. Comparison of total Atlantic OHT with the sum of the overturning and gyre Atlantic OHT components (OHT_{ov}+OHT_{az}) for all models. Solid lines represent the sum of the overturning and gyre Atlantic OHT component and dashed lines represent the total Atlantic OHT.

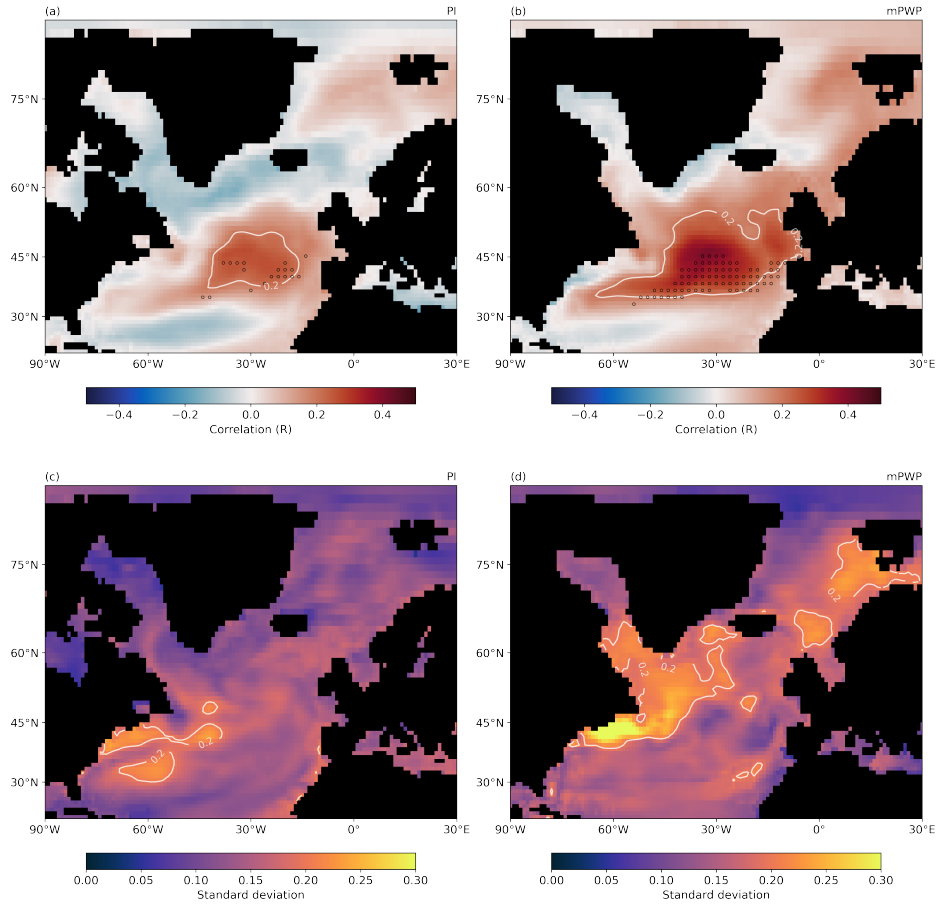

Figure S2. (a) Multi-model mean correlation between the annual AMOC strength and annual SSTs for the pre-industrial simulations. (b) Same as (a) for the mid-Pliocene simulations. Stippling indicates 12 or more models agree on the sign of the correlation. White contours show a positive correlation of $R = 0.2$. (c) Standard deviation from the pre-industrial MMM by individual models. (d) Standard deviation from the mid-Pliocene MMM by individual models. White contours show a standard deviation of 0.2. HadGEM3 is excluded from the MMM and standard deviation calculations.

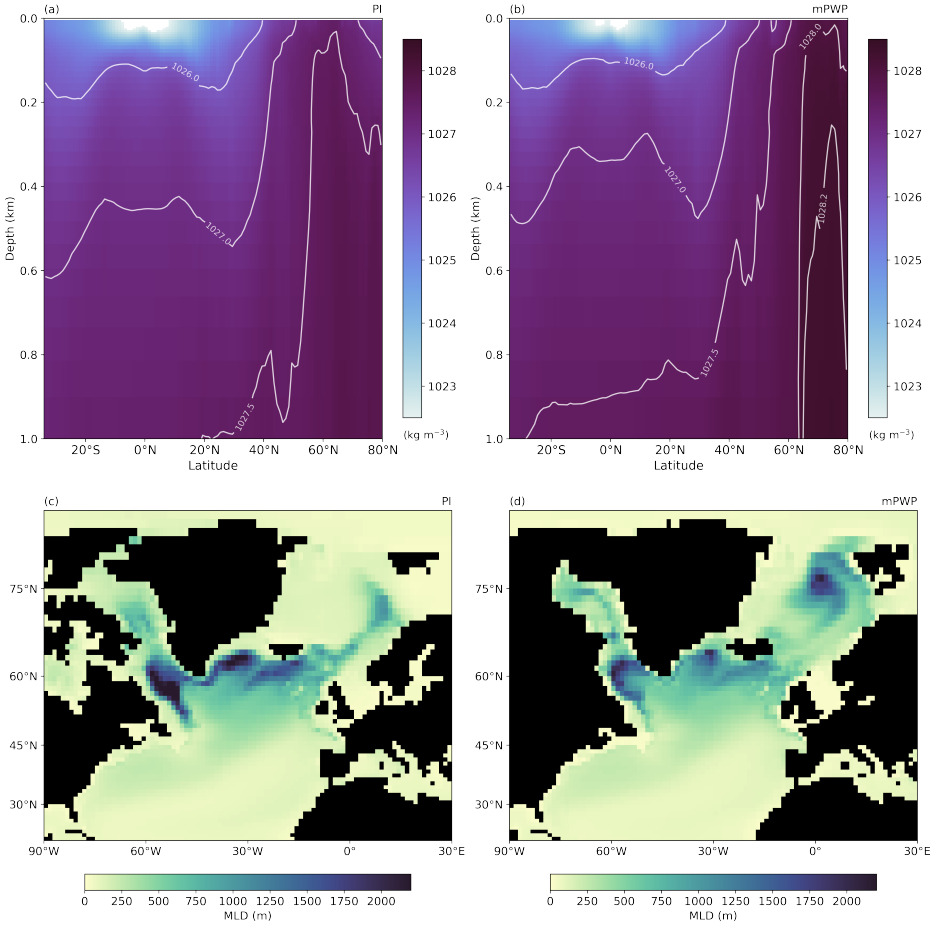

Figure S3. (a) Atlantic zonal mean potential density in top 1 km in the GISS2.1G pre-industrial simulation. (b) Same as (a) for the mid-Pliocene simulation. (c) Average mixed layer depth in the GISS2.1G pre-industrial simulation. (d) Same as (c) for the mid-Pliocene simulation.

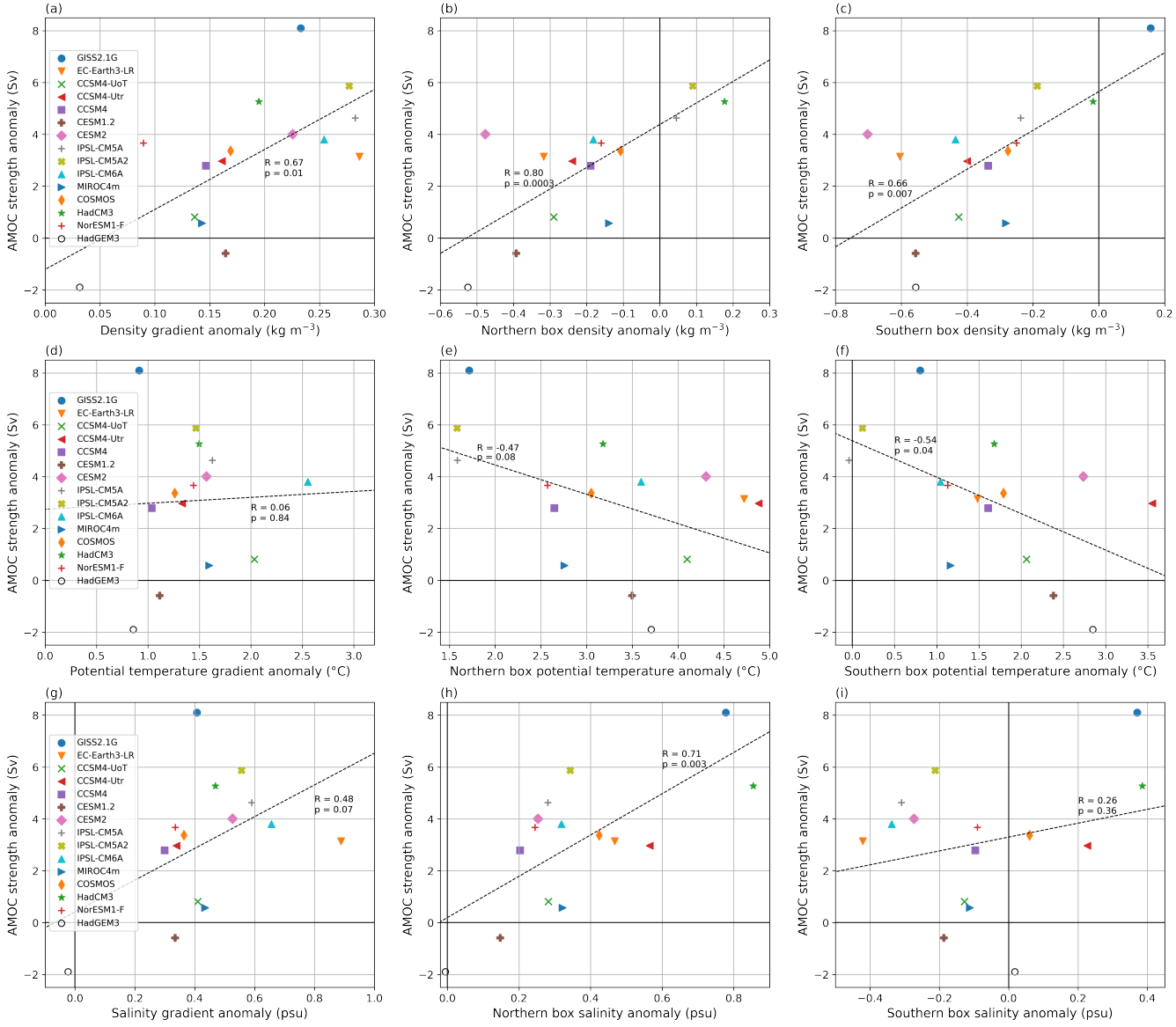

Figure S4. (a) Same as Figure 4c: Individual model mPWP-PI AMOC strength anomaly plotted against the mPWP-PI anomaly in meridional gradient of the top 1 km Atlantic potential density. (b) Individual model mPWP-PI AMOC strength anomaly plotted against the mPWP-PI top 1 km 50-70°N (50-80°N for GISS2.1G) average potential density anomaly. (c) Individual model mPWP-PI AMOC strength anomaly plotted against the mPWP-PI top 1 km 10-30°S average potential density anomaly. (d)-(f) Same as (a)-(c) for potential temperature. (g)-(i) Same as (a)-(c) for salinity. The meridional gradient is defined as the difference between the 50-70°N (50-80°N for GISS2.1G) average and 10-30°S average (latitude bands are indicated by grey shading in Figure 4b).

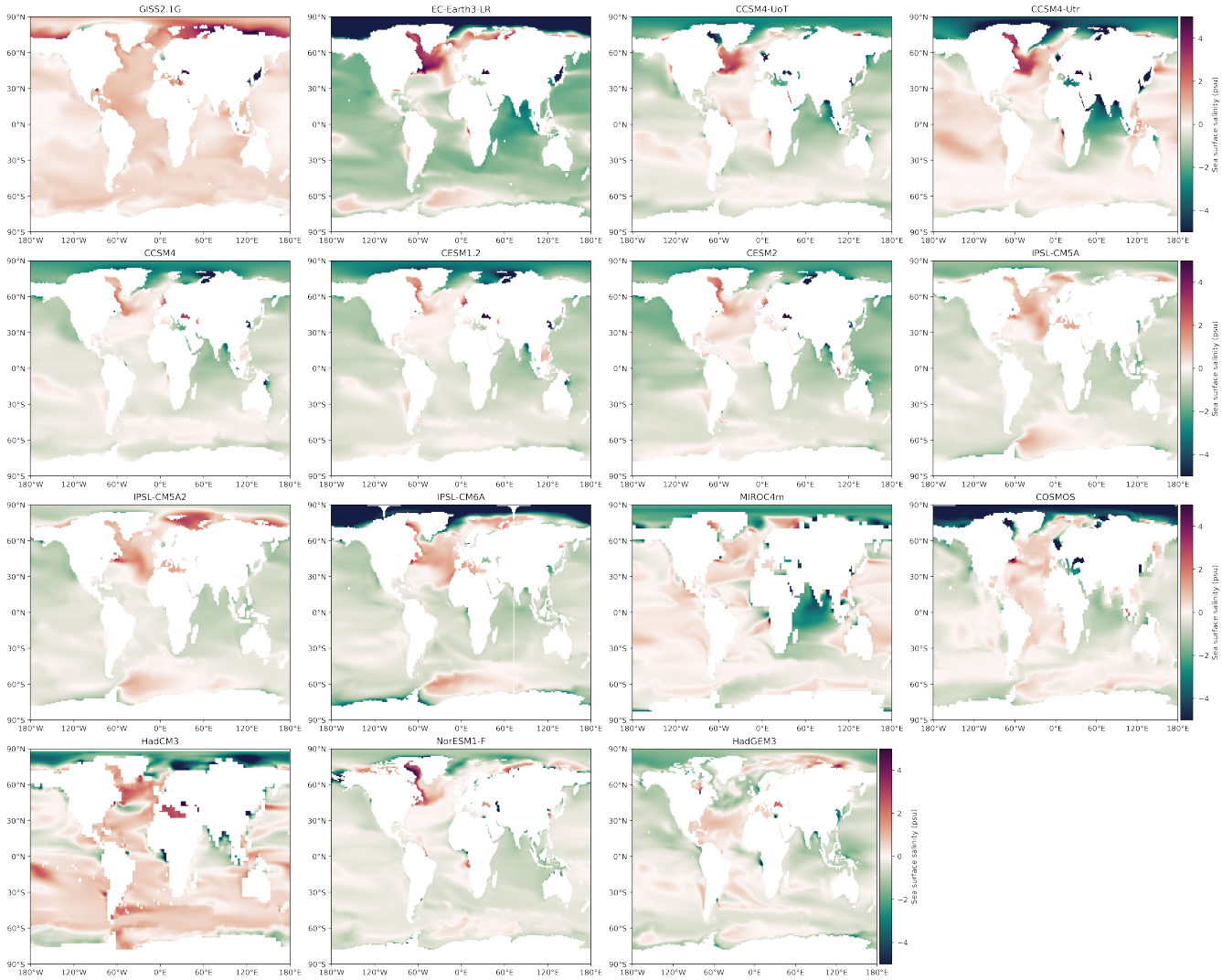

Figure S5. Individual model mPWP-PI difference in sea surface salinity.

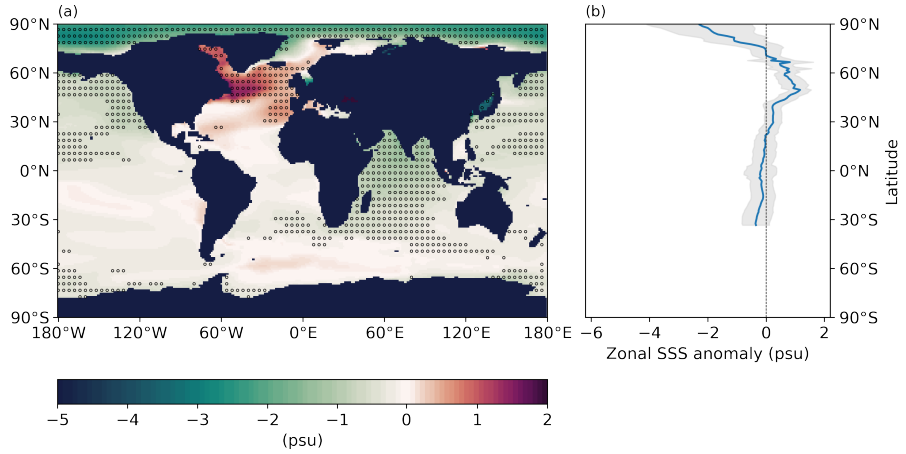

Figure S6. (a) Multi-model mean mPWP-PI difference in top 100 m average salinity. Stippling indicates that 12 or more models agree on the sign of the difference. (b) Atlantic zonal mean salinity difference. The shading indicates one standard deviation from the MMM by individual models, excluding HadGEM3.

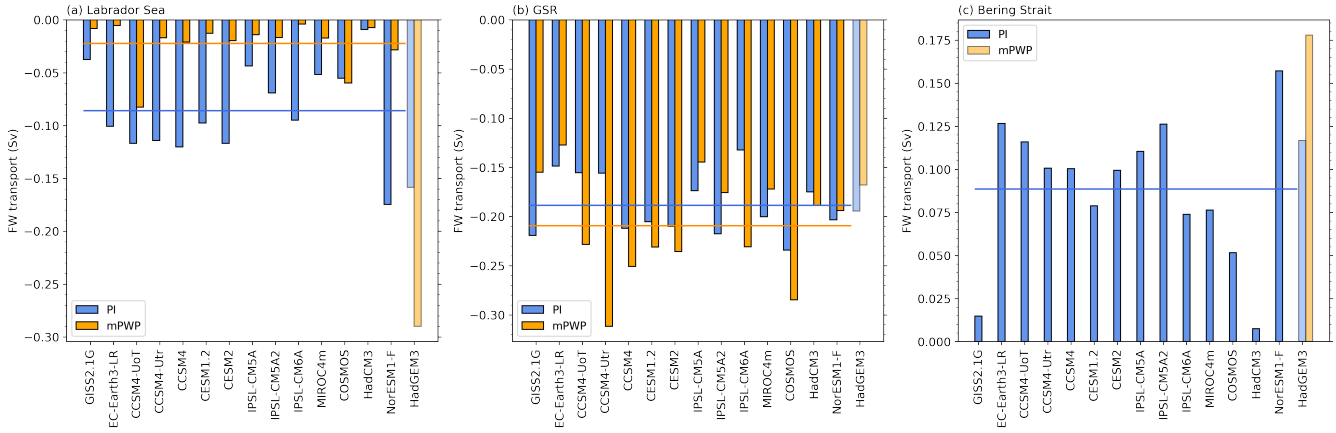

Figure S7. Mean freshwater transport (Sv) in pre-industrial and mid-Pliocene at 62°N (a) into the Labrador Sea and (b) across the GSR. (c) Mean freshwater transport (Sv) through the Bering Strait in the pre-industrial (and mid-Pliocene for HadGEM3). Horizontal lines indicate the MMM transports in the pre-industrial and mid-Pliocene, excluding HadGEM3.

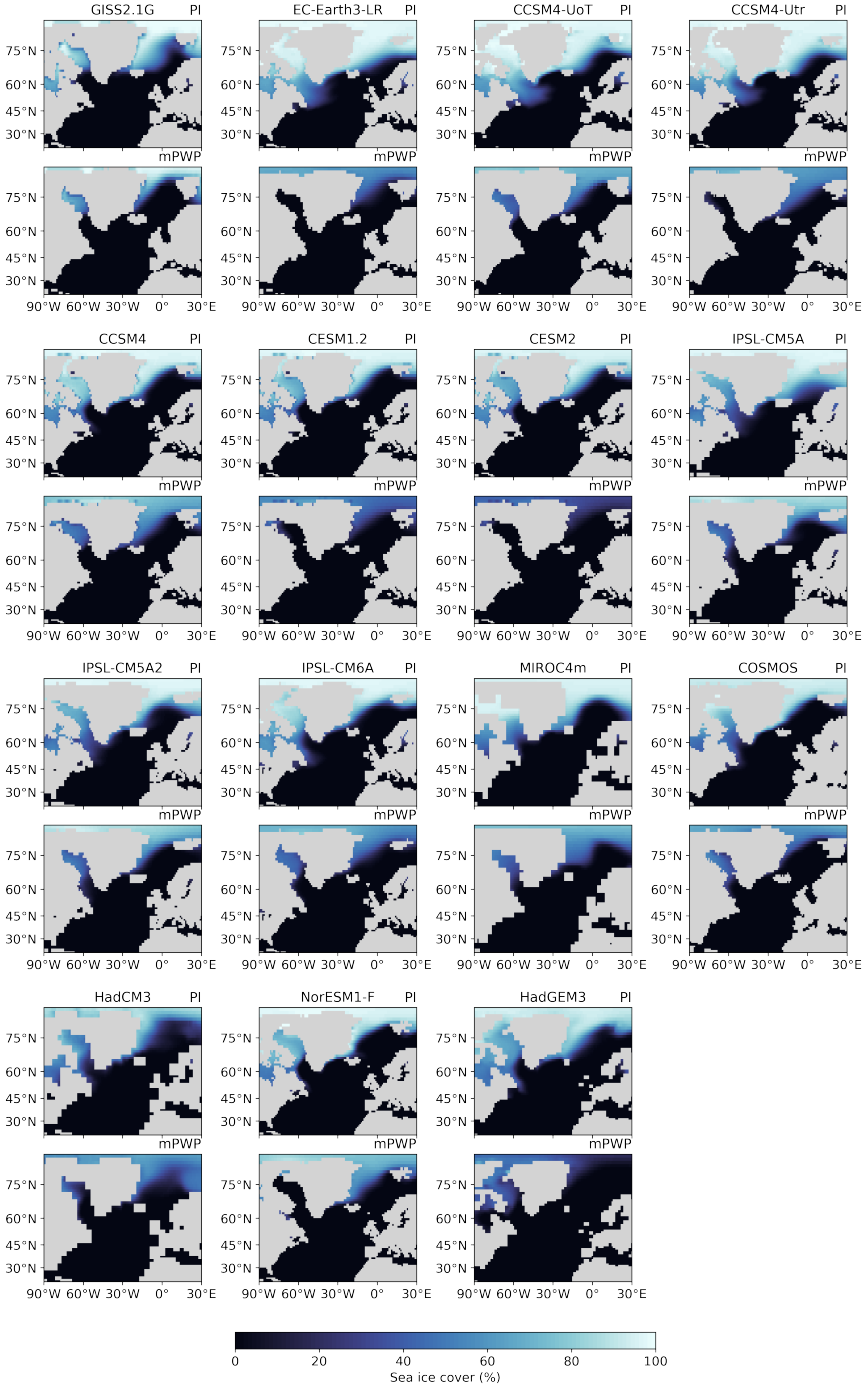

Figure S8. Individual model annual mean sea-ice coverage (%), interpolated to a regular 1x1° grid. The top panel for each model shows the results for the pre-industrial and the bottom panel for the mid-Pliocene. The land-sea masks as shown are not necessarily identical to those of the models due to interpolation.

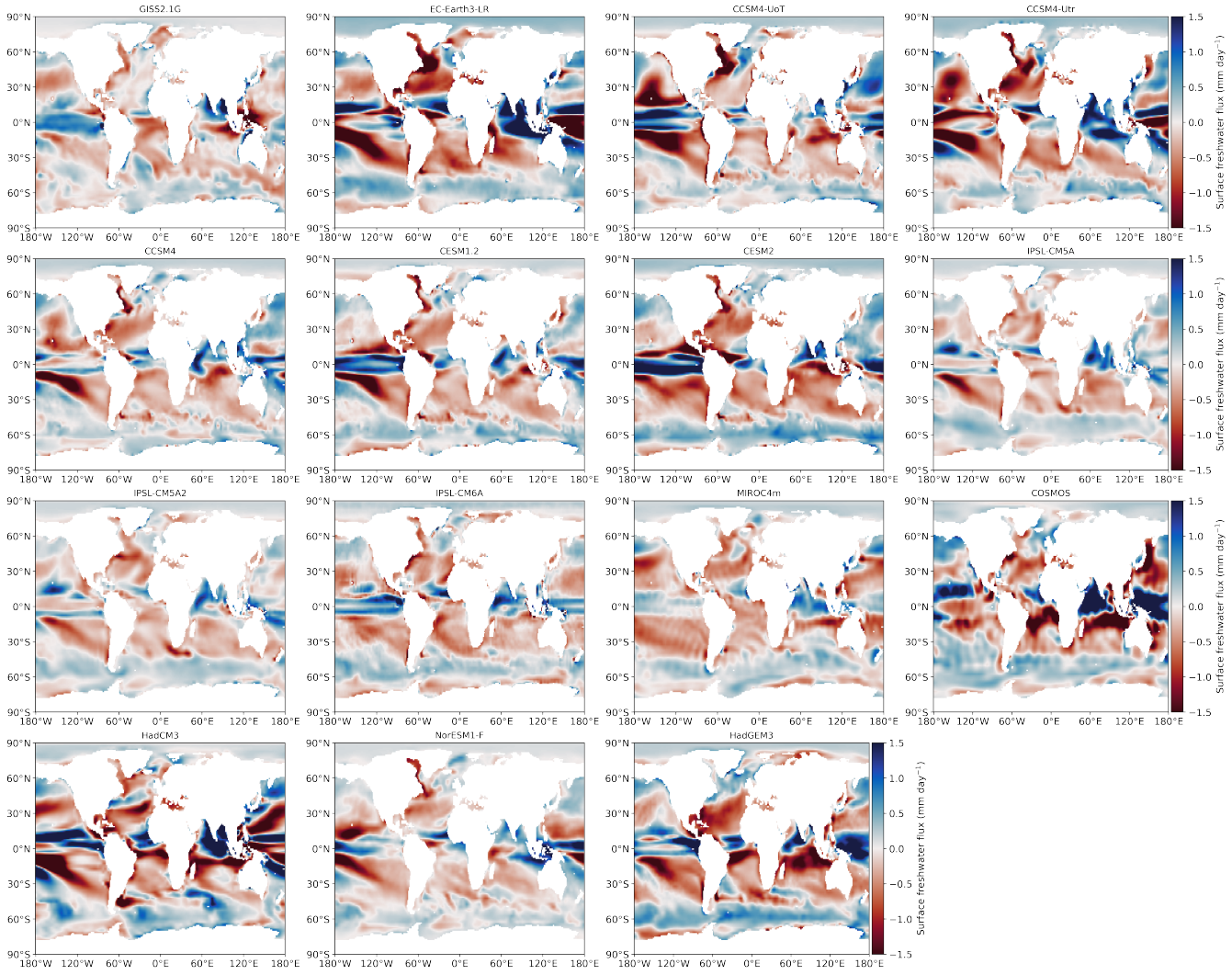

Figure S9. Individual model mPWP-PI difference in surface freshwater flux (PmE).

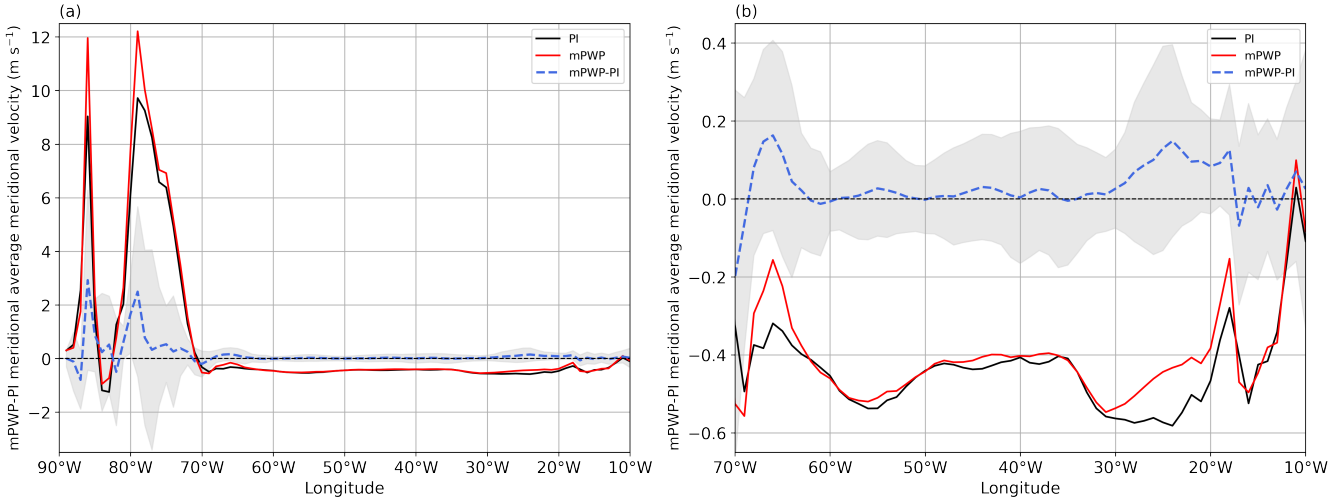

Figure S10. (a) MMM top 500 m Atlantic ocean meridional velocity, averaged over 20-40°N, in the pre-industrial and mid-Pliocene, as well as the mPWP-PI anomaly. Grey shading indicates one standard deviation from the MMM anomaly by individual models. (b) Same as (a) but with adapted scaling to show differences in the 10−70°W longitude band.

Table S1. SST proxy data and MMM at North Atlantic sites. FD19-$U^{k'}_{37}$ refers to the Foley and Dowsett (2019) data, M20-$U^{k'}_{37}$ and M20-Mg/Ca to the McClymont et al. (2020) data. SST proxy mPWP-PI anomalies are computed with pre-industrial ERSST5 data (Huang et al., 2017).

Site	Proxy/MMM	mPWP (°C)	mPWP-PI (°C)	MMM - proxy mPWP (°C)	MMM - proxy mPWP-PI (°C)
603	M20-Mg/Ca	20.4	-1.8	4.7	3.9
	MMM	25.1	2.1		
607/1313	FD19-$U^{k'}_{37}$	21.2	3.4	-1.4	-0.4
	FD19-$U^{k'}_{37}$	20.9	3.1	-1.1	-0.1
	M20-$U^{k'}_{37}$	20.9	3.1	-1.1	-0.1
	M20-$U^{k'}_{37}$	20.3	2.6	-0.5	0.4
	M20-Mg/Ca	22.2	4.5	-2.4	-1.5
	MMM	19.8	3.0		
609	FD19-$U^{k'}_{37}$	18.5	5.1	-3.3	-1.2
	FD19-$U^{k'}_{37}$	17.2	3.8	-2	0.1
	M20-$U^{k'}_{37}$	17.1	3.7	-1.9	0.2
	M20-Mg/Ca	11.7	-1.7	3.5	5.6
	MMM	15.2	3.9		
982	FD19-$U^{k'}_{37}$	17.2	6.5	-2.9	-2.2
	M20-$U^{k'}_{37}$	16.6	5.9	-2.3	-1.6
	MMM	14.3	4.3		
642	FD19-$U^{k'}_{37}$	13.8	7.0	-4.2	-2.9
	M20-$U^{k'}_{37}$	13.2	6.4	-3.6	-2.3
	MMM	9.6	4.1		
907	M20-$U^{k'}_{37}$	3.2	1.7	1.1	2.3
	MMM	4.3	4.0		

Table S2. AMOC-SST correlation map (Figure 3) data. The area of positive correlation is shown as the percentage of significant positively correlated grid cells with respect to the total number of extratropical North Atlantic (30°N-80°N) grid cells. The mean and maximum correlation are respectively the mean and the maximum of all significant positively correlated grid cells in the extratropical North Atlantic.

Model	Area (%)		Mean		Maximum	
	E^{280}	Eoi^{400}	E^{280}	Eoi^{400}	E^{280}	Eoi^{400}
GISS-E2.1G	28	61	0.35	0.38	0.69	0.60
EC-Earth3-LR	1	65	0.25	0.32	0.36	0.54
CCSM4-UoT	30	31	0.34	0.36	0.54	0.62
CCSM4-Utr	11	52	0.28	0.40	0.40	0.72
CCSM4	19	27	0.31	0.27	0.46	0.43
CESM1.2	17	24	0.31	0.31	0.50	0.48
CESM2	40	2	0.35	0.22	0.55	0.26
IPSL-CM6A	32	23	0.36	0.35	0.54	0.56
MIROC4m	9	26	0.27	0.33	0.47	0.55
COSMOS	12	58	0.25	0.39	0.38	0.65
HadCM3	20	52	0.29	0.36	0.49	0.61
NorESM1-F	20	20	0.27	0.29	0.37	0.45
HadGEM3	29	12	0.26	0.29	0.36	0.50
MMM*	20	37	0.30	0.33	0.48	0.54

* HadGEM3 is excluded from the MMM.